Journal of Cerebral Blood Flow & Metabolism (2013) 33, 1259–1269

www.jcbfm.com

ORIGINAL ARTICLE

Signal transduction in cerebral arteries after subarachnoid hemorrhage—a phosphoproteomic approach

Benjamin L Parker[1,2,5], Martin Røssel Larsen[1], Lars IH Edvinsson[3,4] and Gro Klitgaard Povlsen[3]

After subarachnoid hemorrhage (SAH), pathologic changes in cerebral arteries contribute to delayed cerebral ischemia and poor outcome. We hypothesize such changes are triggered by early intracellular signals, targeting of which may prevent SAH-induced vasculopathy. We performed an unbiased quantitative analysis of early SAH-induced phosphorylations in cerebral arteries and evaluated identified signaling components as targets for prevention of delayed vasculopathy and ischemia. Labeled phosphopeptides from rat cerebral arteries were quantified by high-resolution tandem mass spectrometry. Selected SAH-induced phosphorylations were validated by immunoblotting and monitored over a 24-hour time course post SAH. Moreover, inhibition of key phosphoproteins was performed. Major SAH-induced phosphorylations were observed on focal adhesion complexes, extracellular regulated kinase 1/2 (ERK1/2), calcium calmodulin-dependent kinase II, signal transducer and activator of transcription (STAT3) and c-Jun, the latter two downstream of ERK1/2. Inhibition of ERK1/2 6-hour post SAH prevented increases in cerebrovascular constrictor receptors, matrix metalloprotease-9, wall thickness, and improved neurologic outcome. STAT3 inhibition partially mimicked these effects. The study shows that quantitative mass spectrometry is a strong approach to study *in vivo* vascular signaling. Moreover, it shows that targeting of ERK1/2 prevents delayed pathologic changes in cerebral arteries and improves outcome, and identifies SAH-induced signaling components downstream and upstream of ERK1/2.

Journal of Cerebral Blood Flow & Metabolism (2013) **33,** 1259–1269; doi:10.1038/jcbfm.2013.78; published online 29 May 2013

Keywords: cerebral arteries; ERK1/2; phosphoproteomics; STAT3; subarachnoid hemorrhage

INTRODUCTION

Subarachnoid hemorrhage (SAH) inflicts disability and death on thousands of individuals each year. Subarachnoid hemorrhage is associated with two phases of reduced cerebral blood flow (CBF), each of which may cause severe brain damage. In the acute phase, spasmogens in the extravasated blood induce cerebral vasoconstriction for up to several hours. In the delayed phase occurring several days later in around 40% of SAH patients, a complex cerebral vasculopathy develops and contributes to a prolonged CBF reduction.[1]

Cerebral vasculopathy after SAH involves multiple factors including cerebral vasospasm,[1] vascular inflammation,[2] endothelial dysfunction,[3] and upregulation of vasoconstrictor receptors,[4] but the underlying molecular mechanisms are far from fully understood. We hypothesize that intracellular signals activated in cerebral arteries soon after SAH trigger a range of protein expression changes involved in the later vasculopathy. Thus, early intracellular cerebrovascular signals after SAH, hitherto receiving little attention, may hold a key to novel effective treatments for delayed cerebral vasculopathy and ischemia after SAH.

A number of recent studies have explored the therapeutic potential of inhibitors of common intracellular signaling components like protein kinase C,[5] Ras,[6] extracellular regulated kinase 1/2 (ERK1/2),[7] c-Jun, N-terminal kinase,[8] and p38[9] in SAH. However, these studies focus on single signaling pathways studied several days after SAH. Unbiased global studies of cerebrovascular signaling early after SAH and its role in delayed vasculopathy have not been performed.

Quantitative mass spectrometry (MS) has emerged as the method of choice to investigate cell signaling pathways and other intracellular events regulated by phosphorylation in a global and unbiased fashion. More than 100,000 phosphorylation events have been identified by MS and the combination of stable isotope labeling, advances in phosphopeptide enrichment techniques, MS and data reporting standardization has enabled sensitive quantification of phosphorylation changes in complex tissue samples.[10] This is exponentially increasing our understanding of signaling in health and disease.

In this study, we performed an MS-based phosphoproteomic analysis on cerebral artery tissue early after SAH, demonstrating that this is a strong methodology for dissection of acute *in vivo* signaling events in vascular tissue. Selected SAH-induced signaling events identified by MS were validated by immunoblotting, and monitored over a time course of 24 hours post SAH. Moreover, pharmacological inhibition of key signaling events was performed and the effects on other signaling components, delayed cerebrovascular upregulation of vasoconstrictor receptors and

[1]Department of Biochemistry and Molecular Biology, University of Southern Denmark, Odense, Denmark; [2]Discipline of Pathology, School of Medical Sciences, University of Sydney, New South Wales, Australia; [3]Department of Clinical Experimental Research, Glostrup Research Institute, Copenhagen University Hospital Glostrup, Glostrup, Denmark and [4]Division of Experimental Vascular Research, Department of Clinical Sciences, Lund University, Lund, Sweden. Correspondence: Dr GK Povlsen, Department of Clinical Experimental Research, Glostrup Research Institute, Glostrup University Hospital, Nordre Ringvej 69, DK-2600 Glostrup, Denmark.
E-mail: grklpo01@regionh.dk
This work was supported by the Lundbeck Foundation (MRL – Junior Group Leader Fellowship, GKP – Post doc grant, LE – Grant of Excellence), Danish Natural Science Research Council and The University of Sydney Grants-in-aid.
[5]Current address: Diabetes and Obesity Program, Garvan Institute of Medical Research, New South Wales, Australia.
Received 18 January 2013; revised 17 April 2013; accepted 21 April 2013; published online 29 May 2013

matrix metalloprotease-9 (MMP-9), cerebrovascular wall thickness, and neurologic outcome were investigated.

MATERIALS AND METHODS

SAH and Treatments

All experiments were performed in accordance with national guidelines and regulations for use of experimental animals and were approved by the Danish Experimental Animal Inspectorate (approval no.2011/561-2025).

Male Sprague-Dawley rats (300 to 350 *g*) were anesthetized using 3.5% isoflurane (Abbott Laboratories, Abbott Park, IL, USA) in atmospheric air/O_2 (70:30). Rats were orally intubated and kept on artificial ventilation with inhalation of 1% to 2% isoflurane in N_2O/O_2 (70:30) during the surgical procedure. Respiration was monitored by regularly withdrawing blood samples to a blood gas analyzer (Radiometer, Copenhagen, Denmark). Body temperature was maintained at 37°C by a homeothermic heating pad regulated by a rectal temperature probe. Mean arterial blood pressure was measured via a tail artery catheter and intracranial pressure was measured via a catheter placed in cisterna magna. On the right side of the skull, 4 mm anterior from the bregma and 3 mm to the midline, a hole was drilled through the bone to the dura mater without perforation and a laserDoppler probe was placed to measure CBF.

A 27 G blunt cannula with a side hole facing right was stereotactically placed 6.5 mm anterior to the bregma in the midline at an angle of 30° to the vertical plane, placing the tip of the needle just in front of the chiasma opticum. After 30 minutes of equilibration, 250 μL of blood was withdrawn from the tail catheter and injected into the prechiasmatic cistern at a pressure equal to mean arterial blood pressure. Subsequently, rats were maintained under anesthesia for another 60 minutes to allow the animal to recover. The intracranial pressure catheter was cut and sealed with a removable plug 2 cm from the tip. The tail catheter, the needle, and the laser-Doppler probe were removed and incisions closed. Rats were revitalized and extubated. At the end of surgery and every 24 hours until termination, rats received a subcutaneous injection of Carprofen (4 mg/kg) (Pfizer, Ballerup, Denmark) and 10 ml of isotonic saline subcutaneous for hydration. Sham-operated rats went through the same procedure with the exception that no blood was injected intracisternally.

One hundred and six rats were utilized for this study. For MS, 20 rats (10 sham and 10 SAH) terminated 1 hour post surgery and 20 rats (10 sham and 10 SAH) terminated 0.5 hour post surgery were used. Table 1 lists the numbers of animals used in follow-up studies of selected phosphoproteins and treatment with signal transduction inhibitors.

U0126 and KN93 for short-term treatment (up to 12 hours post SAH) were given as 25 μL of 10^{-4} mol/L solutions in isotonic saline with 1% DMSO. For longer-term treatments, U0126 was given as 25 μL of a 10^{-5} mol/L solution and STAT3 inhibitor (STAT3 inhibitor IV cell-permeable peptide, Calbiochem) as 25 μL of a 0.25 10^{-2} mol/L solution, both in saline + 0.1% DMSO. All treatments were given intrathecally into cisterna magna. Timing of the treatments are given in Table 1.

Cerebral Artery Tissue Lysis and Peptide Preparation

Cerebral arteries (basilar artery, middle cerebral arteries, and Circle of Willis) were isolated by dissection and carefully cleared for connective tissue and blood. The tissue was snap frozen in isopentan on dry ice and stored at −80°C. Lysis buffer (0.1 mol/L Na_2CO_3 with phosphatase and protease inhibitors) was added, samples were sonicated, incubated on ice with shaking for formation of membrane microsomes, and ultracentrifuged at 100,000 *g* at 4°C to pellet membrane fraction. Supernatant (cytosolic fraction) was removed and pellet resuspended in 6 mol/L urea, 2 mol/L thiourea, 50 mmol/L triethylammonium bicarbonate, and 1% SDS.

Proteins (in either cytosolic or membrane fractions) were precipitated with trifluoroacetic acid (TFA) and protein pellets resuspended in 6 mol/L urea, 2 mol/L thiourea, 50 mmol/L TEAB, pH 8.0, and reduced with 10 mmol/L dithiothreitol for 1 hour at 25°C and alkylated with 25 mmol/L iodoacetamide for 1 hour at 25°C in the dark. The reaction was diluted 1:10 with 50 mmol/L TEAB, and an aliquot was removed for protein concentration determination using Qubit (Life Technologies Europe BV, Naerum, Denmark). Protein was digested with trypsin (50:1 substrate:enzyme) for 16 hours at 30°C, acidified to 2% (v/v) formic acid, centrifuged at 12,000 × *g* for 15 minutes and the peptide containing supernatant removed.

Peptides were quantified with Qubit (Invitrogen) and 62 μg or 25 μg of peptide from cytosolic and membrane groups, respectively, was labeled with isobaric tags for relative and absolute quantification (iTRAQ; Life Technologies) according to manufacturer's instructions. The reaction mixtures for each group were mixed 1:1:1 and an aliquot checked by MALDI-TOF/TOF-MS (data not shown).

Phosphopeptide Enrichment

The labeled peptides were diluted 10-fold with TiO_2 Loading Buffer (1 mmol/L glycolic acid in 80% ACN, 5% TFA). This solution was incubated with 3 mg TiO_2 beads for 15 minutes at room temperature with gentle agitation. The suspension was then centrifuged at 1,000 × *g* for 1 minute. The supernatant was removed and the beads washed with TiO_2 loading buffer. The suspension was centrifuged at 1,000 × *g* for 1 minute. The supernatant was removed and the beads washed with Washing Buffer 1 (80% ACN, 2% TFA) and centrifuged at 1,000 × *g* for 1 minute. The supernatant was removed and the beads washed with Washing Buffer 2 (20% ACN, 0.2% TFA) and centrifuged at 1,000 × *g* for 1 minute. The supernatant was removed and the modified peptides eluted with 1% ammonium hydroxide, pH 11.3 by vortexing for 15 minutes followed by centrifugation at 1,000 × *g* for 1 minute. The supernatant was removed, acidified to 10% formic acid, 0.1% TFA, and the phosphopeptides purified using a C18/POROS Oligo R3 reversed phase micro-column as described previously,[11] dried by vacuum centrifugation, and stored at −20°C.

TSK Amide-80 Hydrophilic Interaction Liquid Chromatography Peptide Fractionation

Peptide fractionation was performed as described previously.[12] Briefly, peptides were resuspended in 90% MeCN, 0.1% TFA, and loaded onto a 450 μm OD x 320 μm ID x 17 cm microcapillary column packed with TSK Amide-80 (3 μm; Tosoh Bioscience, San Francisco, CA, USA) using an Agilent 1200 Series HPLC (Agilent, Santa Clara, CA, USA). The HPLC gradient was 100% to 60% solvent B (A = 0.1% TFA; B = 90% MeCN, 0.1% TFA) in 30 minutes at a flow rate of 6 μL/minute. Fractions were collected every 1 minute and combined into 10 fractions depending on the intensity of UV

Table 1. Experimental groups receiving treatment

Experimental group	*N*[a] *(N)*	*Time point (hours pre- or post SAH)*[b]							
		1 hour pre	*SAH*	*1 hour post*	*6 hours post*	*12 hours post*	*24 hours post*	*36 hours post*	*48 hours post*
Immunoblotting for selected phosphosites									
1 hour post SAH	5 (15)	V/U/K	V/U/K	†,c					
6 hours post SAH	4 (12)			V/U/K	†				
24 hours post SAH	4 (12)				V/U/K	V/U/K	†		
Effect of MEK1/2 and STAT3 inhibitors on cerebrovascular changes and neurologic outcome									
48 hours post SAH	6 (18)				V/U/S	V/U/S	V/U/S	V/U/S	†

K, KN93; S, STAT3 inhibitor; U, U0126; V, Vehicle.
[a]*N* is the number of rats in each treatment subgroup and (N) is the total number of rats for each time-point of termination. [b]For each group; time points for administration of treatments are indicated. [c,†]Indicates termination of all rats in the group.

detection measured at 210.8 nm. Fractions were dried by vacuum centrifugation.

Nano-Reversed Phase Liquid Chromatography–Electrospray Ionization–Tandem Mass Spectrometry

Fractionated peptides were resuspended in 0.1% formic acid and separated by reversed phase chromatography on an in-house packed 17 cm × 75 μm Reprosil-Pur C18-AQ column (3 μm; Dr Maisch GmbH, Ammerbuch-Entringen, Germany) using an Easy-LC nanoHPLC (Proxeon, Odense, Denmark). The HPLC gradient was 0% to 40% solvent B (A = 0.1% formic acid; B = 90% acetonitrile, 0.1% formic acid) for 120 minutes at a flow of 250 nL/minute. Mass spectrometric detection was achieved using an LTQ-Orbitrap Velos (Thermo Fisher Scientific, Waltham, MA, USA). An MS scan (400 to 2,000 *m/z*; MS AGC = 1×10^6) was recorded in the Orbitrap set at a resolution of 30,000 at 400 *m/z* followed by data-dependent HCD MS/MS analysis of the seven most intense ions with detection in the Orbitrap. Parameters for acquiring HCD were as follows; activation time = 1 millisecond, normalized energy = 48, dynamic exclusion = enabled with repeat count 1, resolution = 7,500, exclusion duration = 30 seconds, injection time = 500 milliseconds and MS^n AGC = 2×10^5.

Analysis of Mass Spectrometry Data

Raw data generated were processed using Proteome Discoverer v1.2beta (Thermo Fisher Scientific) into .mgf files and searched against the IPI rat database v3.76 using the MASCOT program (v1.12). Database searches were performed with the following fixed parameters: precursor mass tolerance of 10 p.p.m., product ion mass tolerance of 0.02 Da, carboxyamidomethylation of Cys, and 1 missed cleavage. Searches were also conducted with the following variable modifications: oxidation of Met; iTRAQ labeling of N-terminus and Lys; phosphorylation of Ser, Thr, Tyr; Quantification was performed using Proteome Discoverer with HCD MS/MS reporter ion integration within a 50 p.p.m. window. All searches were filtered to <1% false discovery rate by searching a reversed-concatenated IPI rat database v3.76. Phosphorylation site localization was aided by the use of a mascot delta score > 8 (ref. 13) combined with manual validation. Peptide ratios were normalized by the median of the unmodified peptides. Intensity-based standard deviations were calculated using a sliding window script developed in R-project.[14] Significant changes were calculated using a $|z\text{-score}| > 1.96$ representing a 95% confidence level.[15]

Western Blotting

The basilar artery (BA) and both MCAs were isolated, cut to a length of exactly 4 mm each, snap frozen as one pooled sample for each rat and lysed in 70 μL boiling LDS sample buffer containing 50 mmol/L dithiothreitol. A total of 20 μL of each sample was separated by 4% to 20% SDS-PAGE (RunBlue, Expedeon, Cambridgeshire, UK) and transferred to a Polyvinylidene difluoride membrane. Membranes were blocked in TBS-T + 5% bovine serum albumin for 1 hour at room temperature and then incubated overnight at 4°C with mouse primary antibodies (see below) followed by incubation with horse-radish peroxidase-conjugated goat anti-mouse IgG antibody (Pierce/Thermo Scientific, Rockford, IL, USA) 1:10,000 for 1 hour at room temperature. Labeled proteins were developed using Lumigen TMA-6 chemiluminiscence solutions (GE Healthcare, Buckinghamshire, UK). Subsequently, membranes were extensively washed in TBS-T and reprobed with rabbit primary antibodies (see below) overnight at 4°C followed by incubation with enhanced chemiluminescence (ECL) horse-radish peroxidase-conjugated donkey anti-rabbit IgG antibody (GE Healthcare) for 1 hour at room temperature and development of labeled proteins. Finally, as a loading control, membranes were washed and reprobed with mouse anti-actin antibodies followed by anti-mouse secondary antibodies as described above. Labeling chemiluminiscence intensities were quantified using the software Image Gauge V4.0 (Fujifilm, Tokyo, Japan) and presented as ratios between band intensities in blots using phosphospecific antibodies and intensities of corresponding bands in blots showing total amounts of the protein.

Primary antibodies: Mouse anti-rat ERK (Cell Signalling Technology, Danvers, MA, USA), mouse anti-rat calcium calmodulin-dependent kinase II (CaMKII) (Abcam, Cambridge, UK), mouse anti-rat focal adhesion kinase (FAK) (BD Biosciences, Albertslund, Denmark), mouse anti-rat STAT3 (Cell Signalling Technology), mouse anti-rat c-Jun (Tocris Biosciences, Abingdon, UK), mouse anti-rat actin (Abcam), Rabbit anti-rat phospho-ERK (Thr202/Tyr204), rabbit anti-rat phospho-CaMKII (Thr286), rabbit anti-rat phospho-FAK (Tyr397), rabbit anti-rat phospho-STAT3 (Ser727), rabbit anti-phospho-STAT3 (Tyr705), rabbit anti-rat phospho-c-Jun (Ser73) (all Cell Signalling Technology), and rabbit anti-rat phospho-FAK (Ser910) (Abcam).

Histology and Immunohistochemistry

Middle cerebral arteries were snap frozen in TissueTek, cryosectioned, and fixed in Steffanini's fixative. Sections were stained with hematoxylin-eosin using a standard protocol. A cross was fixed on the screen and the image moved so the cross was placed in the middle of the vessel. Wall thickness was measured 12, 3, 6, and 9 O'clock in three sections of each vessel and means calculated.

Immunohistochemical assessment of protein expression levels of the 5-HT_{1B} receptor (rabbit, 1:100, ab13896, Abcam, UK), IL-6 (rabbit, 1:400, ab6672, Abcam), and MMP-9 (rabbit, 1:400, ab7299, Abcam) in cerebral arteries was performed using indirect immunohistochemistry. Briefly, the sections were rehydrated for 15 minutes in phosphate-buffered saline (PBS) containing 0.25% Triton X-100 (PBS-T, Merck Millipore, Billerica, MA, USA), and thereafter exposed to primary antisera in PBS-T containing 1% bovine serum albumin overnight in a moist chamber at +4°C. Sections were then rinsed in PBS-T for 2 × 15 minutes followed by incubation with secondary antibodies (Texas Red 1:100 for ET_B, FITC 1:100 for the other primary antibodies, Jackson ImmunoResearch, West Grove, PA, USA) for 1 hour in dark at room temperature. Thereafter, sections were rinsed in PBS-T for 3 × 10 minutes in room temperature and mounted with mounting medium Vectashield containing 4′,6-diamino-2-phenylindole (nucleus staining, Vector Laboratories, Burlingame, CA, USA). Omission of the primary antibody served as negative controls. Sections were examined and images were obtained using epifluorescence microscope (Nikon 80i, Tokyo, Japan) coupled to a Nikon DS-2MV camera. FITC (480/30X), TRITC (540/24X) and 4′, 6-diamino-2-phenylindole (360/40X) filters were used (filter specifications are given in nanometers and X denotes excitation center wavelength/bandwidth). Adobe Photoshop CS3 (v.8.0, Adobe Systems, Mountain View, CA, USA) was used to superimpose the digital images. Localization and cellular pattern of the staining in the vessel wall was evaluated and the intensity of immunohistochemical fluorescence in the smooth muscle layer was graded (from 1 to 3) by an investigator masked towards the experimental groups of the sections.

Rotating Pole Test for Assessment of Neurologic Function

Gross sensorimotor function (integration and coordination of movements as well as balance) was evaluated by the ability of the rats to traverse a rotating pole, which was either steady or rotating at different speeds (3 or 10 r.p.m.). At one end of the pole (45 mm in diameter and 150 cm in length), a cage was placed with an entrance hole facing the pole. The performance of the rat was scored according to the following definitions: score 1, the animal is unable to balance on the pole and falls off immediately, score 2, the animal balances on the pole but has severe difficulties crossing the pole and moves less than 30 cm, score 3, the animal embraces the pole with the paws and does not reach the end of the pole but manages to move more than 30 cm, score 4, the animal traverses the pole but embraces the pole with the paws or jumps with the hind legs, score 5, the animal traverses the pole with normal posture but with more than 3 to 4 foot slips, score 6, the animal traverses the pole perfectly with less than 3 to 4 foot slips.

All rotating pole tests were performed by personnel masked with regard to experimental groups of the animals. Tests were performed in the morning to minimize diurnal rhythm variation and in a silent room with as few visual disturbing elements as possible.

RESULTS

Dissecting Early Subarachnoid Hemorrhage-Induced Phosphorylation Events in Cerebral Arteries by Mass Spectometry

The application of quantitative MS to investigate early SAH-induced signal transduction has not previously been performed and, we hypothesized that this would reveal novel targets for therapeutic intervention. However, since the recovery of protein extracted from dissected cerebral arteries is relatively low (<100 μg for ten pooled animals), the analytical strategy employed had to be carefully considered. To reveal SAH-induced phosphorylation events, we employed iTRAQ-based quantification

and TiO_2 phosphopeptide enrichment combined with hydrophilic interaction liquid chromatography and high resolution tandem MS, providing an effective strategy to monitor hundreds of phosphorylation sites from a low amount of material ($<200\ \mu g$).[12] We used cerebral artery tissue lysates from three groups; sham, 0.5 hours post SAH, and 1 hour post SAH ($n = 10$ for each group). The experiment was performed in biological replicate and included analysis of cytosolic and membrane fractions.

A total of 1,317 unique phosphopeptides were identified at a 1% false discovery rate. A ratio corresponding to the 95% quantile resulted in approximately 1.9-fold change cut-off. However, since the intensity of the observed iTRAQ reporter ions is known to influence quantification precision, i.e., lower signals have higher variability,[16] we used a sliding window script for calculation of the $|z\text{-score}|$, representing the intensity-dependent standard deviation for each phosphosite, and a $|z\text{-score}| > 1.96$ was regarded a significant change.[15] Furthermore, spectrum quality, peptide identification and phosphosite localization for each phosphosite with $|z\text{-score}| > 1.96$ were manually validated in addition to phosphorylation site localization using the mascot delta score. Using this approach, 68 unique phosphosites were found to be significantly regulated in SAH (0.5 hours and/or 1 hour post SAH) compared with sham-operated rats. Table 2 lists the regulated phosphosites, their SAH-induced fold changes (log_2-transformed SAH/sham ratios), and *z*-scores.

Significantly regulated phosphoproteins were assigned to functional groups based on their associated gene ontology terms and available information in the literature (Figure 1 and Table 2). The largest fraction (39.3%) was assigned to focal adhesion-associated proteins. In addition, 13.1% of the regulated phosphoproteins were involved in gene transcription and translation, and another 8.2% were intracellular signaling components, i.e., mainly kinases and phosphatases. Moreover, a number of other cytoskeletal proteins (8.2%) and proteins associated with the dystrophin signalosome (8.2%) were regulated. Finally, proteins involved in more direct regulation of myosin light-chain phosphorylation (9.8%) were regulated, probably reflecting acute SAH-induced vasoconstriction. The majority of the significantly regulated phosphorylation sites shown in Table 2 have not previously been associated with SAH. This highlights the ability of quantitative MS to identify previously uncharacterized phosphorylation events, which may have significant functional roles and be valuable therapeutic targets.

To predict upstream kinases responsible for the SAH-induced phosphorylation events, we performed a kinase motif analysis using the NetworKIN software.[17] A large fraction (21.2%) of the regulated phosphosites resided in the P*X*p(S/T)P mitogen-activated protein kinase MAPK phosphorylation motif (Figures 2A-C), suggesting that many of the SAH-induced phosphorylations are mediated by MAPKs. In our MS analysis, we identified only one MAPK regulated after SAH, namely ERK1, which was increasingly phosphorylated on its two activating phosphosites Thr202 and Tyr204 with a log2-transformed fold change of 2.23 (Figure 2D). However, the *z*-score for this upregulation was below 1.96 (1.2) and it is therefore not included in Table 2. This early SAH-induced ERK1/2 activation was verified by phosphospecific western blotting (Figure 3A), however with large variations in the degree of ERK1/2 phosphorylation between SAH rats, which may explain the low *z*-score in the MS experiments.

In addition to ERK1/2, we selected a number of other significantly regulated kinases and transcription factors for validation by western blotting. These were the CaMKII, the FAK (both known to interact with the ERK1/2 pathway in some cellular contexts[18,19]) and the transcription factors STAT3 and c-Jun (potential downstream mediators of expressional changes involved in the later vasculopathy). We verified SAH-induced phosphorylation of CaMKII at its autophosphorylation site Thr286, indicating CaMKII activation (Figure 3B). We also verified the phosphorylation of FAK at Ser910 (Figure 3C), a regulatory phosphosite with largely unknown functions. In addition, we demonstrated a relatively weak but clearly detectable SAH-induced phosphorylation of FAK at Tyr397, an autophosphorylation site recruiting downstream signaling effectors (Figure 3D). Finally, we verified the observed phosphorylation of STAT3 (Figure 3E) and c-Jun (Figure 3F), on phosphosites known to promote transcriptional activity.[20,21]

Role of Extracellular Regulated Kinase 1/2 and Calcium Calmodulin-Dependent Kinase II in Early Subarachnoid Hemorrhage-Induced Signaling in Cerebral Arteries

The ERK1/2 pathway has earlier been shown to have a central role in delayed expressional changes in cerebral arteries after SAH.[4] To investigate whether our selected panel of SAH-induced phosphorylations occurred downstream of the ERK1/2 pathway, we treated SAH rats with the mitogen-activated protein kinase kinase MEK1/2 (upstream activator of ERK1/2) inhibitor U0126 (Figure 3A). U0126 completely prevented SAH-induced phosphorylation of FAK Ser910, but not at Tyr397 (Figures 3C and 3D). Moreover, U0126 significantly inhibited SAH-induced phosphorylation of STAT3 and c-Jun.

Calcium calmodulin-dependent kinase II has been suggested to have a central role in expressional changes during organ culture of cerebral arteries, sometimes used as an *in vitro* model of cerebrovascular changes in stroke.[22] However, in our panel of selected SAH-induced phosphorylations, CaMKII inhibition only affected phosphorylation of FAK at Tyr397, most likely an indirect effect since CaMKII is a serine-threonine kinase and Tyr397 is a FAK autophosphorylation site.

Time Course of Selected Subarachnoid Hemorrhage-Induced Phosphorylations

Early SAH-induced signals are potential therapeutic targets only if they remain activated within a clinically relevant time-window for administration of pharmacological inhibitors. We therefore investigated the time course of activation of our panel of selected phosphoproteins over the first 24 hours post SAH. Calcium calmodulin-dependent kinase II, FAK, and c-Jun were no longer significantly regulated at 6 hours and 24 hours post SAH (Figures 4B, 4C, 4D, and 4F), indicating that these phosphoproteins are only transiently regulated early after SAH suggesting limited potential as therapeutic targets. In contrast, the ERK1/2 and STAT3 phosphosites remained elevated at 6 hours and 24 hours post SAH (Figures 4A, 4E, 4G, and 4H). STAT3 phosphorylation was strongly inhibited by U0126 at all time points tested.

Role of Extracellular Regulated Kinase 1/2 and Signal Transducer And Activator of Transcription 3 in Cerebral Vasculopathy and Neurologic Deficits after Subarachnoid Hemorrhage

After an SAH, cerebral arteries increase their expression of smooth muscle contractile endothelin B (ET_B) and 5-hydroxytryptamine 1B ($5\text{-}HT_{1B}$) receptors and MMP-9, and early activation of the ERK1/2 pathway has already been shown to be involved in these pathologic gene transcription changes.[4] To investigate whether STAT3 is a downstream mediator of these changes, thereby being a possible alternative to direct therapeutic targeting of the ERK1/2 pathway, we compared the effects of STAT3 and MEK1/2 inhibition on cerebrovascular upregulation of ET_B, $5\text{-}HT_{1B,}$ and MMP-9 at 2 days post SAH. Both treatments were given intrathecally starting 6 hours post SAH, since MEK1/2 inhibition has earlier been shown to effectively prevent SAH-induced vasculopathy in this treatment regimen.[7] Figure 5A shows STAT3 inhibition by the employed STAT3 inhibitor in this treatment regimen.

Treatment with U0126 completely prevented SAH-induced upregulation of ET_B, $5\text{-}HT_{1B,}$ and MMP-9, whereas the STAT3 inhibitor completely prevented upregulation of ET_B and partially

Table 2. Phosphopeptides significantly regulated (*z*-scores > 1.96) in 0.5 hour and/or 1 hour post SAH animals as compared with sham-operated animals

Gene name	*Protein description*	*Phospho site*[a]	*0.5 hour post SAH*		*1 hour post SAH*	
			Fold change	*Z-score*	*Fold change*	*Z-score*
Organization of focal adhesion plaques and the actin cytoskeleton (39.3%)[b]						
PALLD	Palladin	Ser893	3.03	3.46	2.2	4.00
PALLD	Palladin	Ser1392	2.38	2.86	2.47	4.51
NEXN	Nexilin	Ser359	0.9	1.27	2.43	2.88
PTK2	Focal adhesion kinase 1	Ser910	1.7	2.22	2.4	2.59
TPM1/2	Tropomyosin 1/2	Ser87	0.2	0.24	2.3	2.69
VIM	Vimentin	Ser420	1.0	0.94	2.1	3.70
TNS1	Tensin-1	Ser992	1.7	2.36	2.0	2.32
PDLIM1	PDZ and LIM domain protein 1	Thr146	0.4	0.53	2.0	2.04
TNS1	Tensin-1	Ser907	1.7	2.12	1.8	1.7
SPECC1L	Cytospin-A	Ser869	1.74	2.29	1.1	1.13
FLNA	Filamin alpha	Ser968	0.4	0.75	1.5	2.17
TPM1/2	Tropomyosin 1/2	Thr282	−4.3	5.07	−3.40	5.83
TAGLN	Transgelin (SM22)	Ser181	−2.8	4.00	−1.7	2.29
TAGLN	Transgelin (SM22)	Ser186	−2.7	4.09	−1.6	2.20
CSRP3	Cysteine and glycine-rich protein 3 (cardiac LIM domain protein)	Ser95	−0.2	0.41	−2.6	3.00
CSRP1	Cysteine and glycine-rich protein 1	Ser81	−2.1	3.09	0.0	0.19
VASP	Vasp protein	Thr327	−2.0	2.60	−0.8	1.08
TAGLN	Transgelin (SM22)	Thr164	−1.9	2.55	−0.8	1.09
SMTN	Smoothelin	Ser138	−1.7	2.24	−1.1	1.91
HSPB6	Heat shock protein beta-6	Ser16	−1.7	2.44	−0.9	1.26
TNS1	Tensin-1	Ser1295/6	−1.57	2.08	−0.94	1.27
SMTN	Smoothelin	Ser299	−1.5	2.35	0.1	0.03
LMOD1	Leiomodin 1	Ser119	−1.4	2.11	−0.2	0.43
LMOD1	Leiomodin 1	Ser87	−1.2	2.21	−0.1	0.43
Regulation of gene transcription and translation (13.1%)						
EIF4B	Eukaryotic translation initiation factor 4B	Thr500	1.6	2.03	2.3	2.43
ZYX	Zyxin	Ser336	1.8	2.36	1.9	2.05
HMGN1	High-mobility group nucleosome binding domain 1 (HMGN1)	Ser6	1.4	2.04	1.9	2.38
JUN	c-Jun	Ser73	1.3	0.70	1.8	2.05
ZFP36	Tristetraproline	Ser59	1.1	1.29	1.7	2.36
STAT3	Signal transducer and activator of transcription 3	Ser727	1.0	0.99	1.6	2.94
RPLP1	60S acidic ribosomal protein P1	Ser101, Ser104	0.78	0.97	−6.8	7.82
TRIM28	Transcription intermediary factor 1-beta (KAP1)	Ser51	−1.0	1.34	−1.72	2.08
Regulation of contraction (myosin light chain phosphorylation) (9.8%)						
MPRIP	Myosin phosphatase Rho-interacting protein (MRIP)	Ser622	2.0	2.78	2.6	3.05
PPP1R12C	Protein phosphatase 1, regulatory subunit 12C	Ser508	0.8	0.8	1.2	2.28
MURC	Muscle-related coiled-coil protein	Ser20	0.6	0.67	−6.8	7.68
ARHGEF7	Rho guanine nucleotide exchange factor 7c (Beta-pix 7c)	Ser340	−1.7	2.01	0.0	0.17
PPP1R12A	Protein phosphatase 1 regulatory subunit 12A (MYPT1)	Ser601	−1.4	2.07	−0.1	0.27
PPP1R14A	Protein phosphatase 1 regulatory subunit 14A	Ser26	−1.3	2.08	0.3	0.24
Intracellular signaling (8.2%)						
CAMK2G	Calcium/calmodulin-dependent protein kinase typell subunit gamma	Thr286	1.9	2.38	−0.2	0.11
PP1R1A	Protein phosphatase 1 regulatory subunit 1A	Ser67	1.5	2.13	0.3	0.20
PRPF4B	Serine/threonine-protein kinase PRP4 homolog	Ser43, Ser45	0.2	0.40	−2.5	2.88
SORBS2	Sorbin/ArgBP2	Ser325	−2.1	2.88	−0.3	0.57
PRKCDBP	Protein kinase C delta-binding protein (Cavin-3)	Ser199	−0.8	1.02	−2.0	2.39
Components of the dystrophin glycoprotein complex (8.2%)						
SYNM	Desmuslin (Synemin)	Ser1144	0.9	1.16	2.3	2.34
DTNA	Dystrobrevin alpha isoform 7	Ser609	1.8	1.90	1.1	2.05
SNTA1	Syntrophin alpha 1	Ser194	1.8	2.04	0.99	1.96
DMD	Dystrophin isoform Dp71a	Thr340	−1.7	2.12	−2.35	2.75
PTRF	Polymerase I and transcript release factor (Cavin-1)	Ser302	−1.4	2.02	−0.6	0.96
Other cytoskeletal components (8.2%)						
LMNA	Lamin-A	Ser257	1.9	2.31	1.4	1.59
TNKS1BP1	Tankyrase 1-binding protein of 182 kDa	Ser1125	1.7	2.19	1.6	2.41
SRRM2	Serine/arginine repetitive matrix 2	Ser1151	1.6	2.24	−0.3	0.52
DES	Desmin	Ser28, Ser31	1.2	1.19	1.4	2.53
MAP4	Microtubule-associated protein 4	Ser902	−1.5	2.19	−1.1	1.54
Miscellaneous (13.1%):						
SLC4A1	Anion exchange protein 1	Ser18	1.9	2.00	1.4	2.48
TRIM47	Tripartite motif-containing 47	Ser592	1.4	1.79	1.88	2.87
PDHA1	Pyruvate dehydrogenase E1 component	Ser232	1.6	2.26	1.5	1.77
CGNL1	Cingulin-like protein 1	Ser251	1.2	1.29	1.06	2.05
IER3	Immediate early response 3	Ser31	1.0	0.97	1.1	2.07
MB	Myoglobin	Tyr120	0.5	0.53	−6.8	7.69
NDRG2	N-myc downstream regulated gene 2 (NDRG2 protein)	Ser318, Thr320	1.1	1.38	−1.8	2.27
SMAP	Small acidic protein	Ser17	−0.5	0.77	−1.7	2.16

[a]Amino acids are numbered according to UniProt numbering. [b]Phosphosites are divided into categories according to the main known cellular function of the protein on which they reside. Within each category, phosphosites are ordered after highest fold changes, with all positively regulated sites within the category presented first followed by all negatively regulated sites.

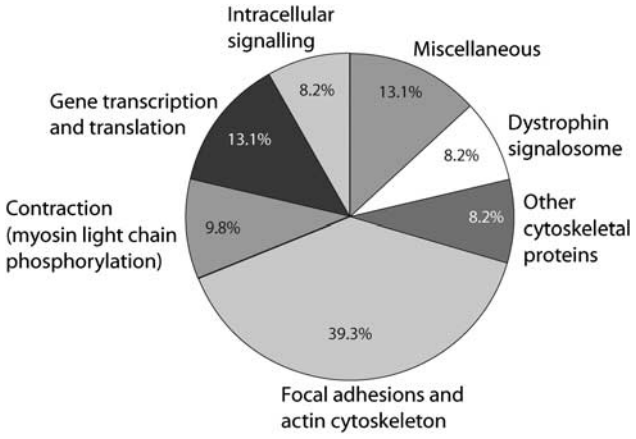

Figure 1. Cellular functions of regulated phosphoproteins. All subarachnoid hemorrhage-regulated phosphosites were manually grouped in functional categories according to the main known cellular function of the protein on which they reside. Percentages indicate fractions of the total number of regulated sites.

prevented upregulation of MMP-9, but had no effect on the SAH-induced upregulation of 5-HT_{1B} (Figure 5B). This suggests that STAT3 is a downstream mediator of some, but not all, SAH-induced cerebrovascular expressional changes mediated by MEK–ERK1/2 signaling.

The smooth muscle layer of cerebral arteries undergoes thickening after SAH as a result of vasoconstriction, inflammation, and/or structural remodeling of the vascular wall (Figures 5C and 5D). We found that this vascular wall thickening evident at 2 days post SAH was reduced by U0126 treatment but not by the STAT3 inhibitor (Figures 5C and 5D). Finally, treatment with U0126 significantly improved neurologic function of the rats at 48 hours post SAH assessed by a rotating pole test, whereas treatment with STAT3 inhibitor had no significant effect in this test.

DISCUSSION

The present study is, to our knowledge, the first quantitative phosphoproteomics analysis of *in vivo* phosphorylation events in vascular tissue and the only large scale quantitative phosphoproteomic analysis of signaling associated with SAH. We used this approach to dissect early SAH-induced phosphorylation events in cerebral arteries with the goal of identifying possible triggers of later expressional changes involved in SAH-induced vasculopathy and delayed cerebral ischemia. Based on the quantitative phosphoproteomics data we show; (1) predominant hitherto unrecognized acute SAH-induced regulation of focal adhesion complexes and actin cytoskeleton dynamics, including activation of FAK, (2) a central role of early cerebrovascular activation of ERK1/2, which acts as an upstream kinase mediating a large number of early SAH-induced phosphorylation events and has a central role in the later development of cerebral vasculopathy and neurologic deficits, (3) STAT3 is a downstream transcription factor mediating some, but not all, vasculopathological changes induced by ERK1/2 signaling after SAH.

A large research effort has been invested in studying and targeting individual aspects of the complex vasculopathy after SAH, e.g., with vasoconstrictor receptor antagonists and anti-inflammatory drugs,[23,24] but without clinical success. To observe clinical effect, it may be necessary to target a broad range of the pathologic processes in the cerebral vasculature. One possible strategy is to target early signaling events that trigger later expressional changes in proteins involved in the vasculopathy. However, most studies of the role of intracellular signals in SAH-induced vasculopathy have been performed at delayed time points where the initial triggering events may have decayed. Furthermore, those studies investigating the intracellular signals have taken a reductionist approach and only studied a handful of signaling molecules (e.g., kinases) and not identified the functional targets of phosphorylation from a systems wide perspective.

Global proteomic analyses of protein expression changes in diseased vascular tissue have recently been performed,[25,26] but to our knowledge, phosphoproteomics in native vascular tissue has not been performed earlier. We here demonstrate that this is a strong approach, feasible even when studying acute *in vivo* phosphorylations using small starting amounts of vascular tissue. The fact that we were able to validate the identified SAH-induced regulation of all phosphosites selected for follow-up analysis, underscores the validity of the phosphoproteomic method. Phosphoproteomic methods beyond those presented in the present study could be applied to further investigate signal transduction after SAH. For example, the activation of kinases could be measured using MS-based multiplexed kinome activity assays.[27] Furthermore, the kinases mediating the majority of the phosphorylation sites identified in the present study are unknown. Recent advances in multiplexed *in vitro* kinase assays using peptide libraries and MS are exponentially increasing our understanding kinase–substrate relationships.[28] The combination of the present study with further MS-based assays to characterize kinase activities and targets will undoubtedly increase our understanding of SAH-induced signal transduction.

Our analysis uncovered a substantial SAH-induced regulation of proteins associated with focal adhesions. These complexes integrate biochemical and mechanical stimuli, including shear force, cyclic stretch, and contractile state of the vascular wall, into intracellular signals and changes in actin cytoskeleton dynamics, with FAK as a key activator of downstream signals.[29] We demonstrate for the first time regulation of FAK in cerebral arteries after SAH both at the autophosphorylation site Tyr397, indicating kinase activation, and at the regulatory phosphosite Ser910, the latter mediated by ERK1/2 in accordance with earlier studies.[30,31] Other examples of identified SAH-regulated focal adhesion proteins are Tensin-1 and PDZ and LIM domain protein 1, both linkers between signaling pathways and the cytoskeleton.[32,33] We classified 39.3% of the SAH-regulated phosphosites to focal adhesions, however this may be an underestimate since some proteins assigned to other functional groups are also known to be involved in focal adhesion-mediated signaling, such as the transcription factor Zyxin[34] and the adapter protein Sorbin.[35]

FAK is known to be regulated by a variety of mechanical and biochemical stimuli.[29] We speculate that the dramatic changes in hemodynamic forces acting on the vascular wall during acute SAH may induce FAK activation. Interestingly, a recent study from our laboratory demonstrated that the lack of vascular wall tension during organ culture of cerebral arteries induces smooth muscle FAK activation and downstream ERK1/2 activation, which again induces upregulation of contractile ET_B receptors.[36] In support of a similar series of events in SAH, inhibition of the downstream FAK effector Src reduced cerebrovascular ERK1/2 activation and cerebral vasospasm after SAH in dogs.[37]

The involvement of early MEK-ERK1/2 activation in later cerebrovascular changes after SAH has been demonstrated in several earlier studies.[4,6,7] The present study confirms this role and demonstrates broad and multifactorial beneficial effects of early MEK1/2 inhibition in SAH, including prevention of cerebrovascular ET_B, 5-HT_{1B}, and MMP-9 upregulation and cerebrovascular wall thickening. We suggest that the combination of these vascular effects together restores CBF and leads to improved neurologic outcome. Interestingly, administration of the MEK1/2 inhibitor could be delayed 6 hour post SAH and still have these effects. Thus, early MEK1/2 inhibition prevents multiple detrimental processes within a clinically realistic time-window, and thus

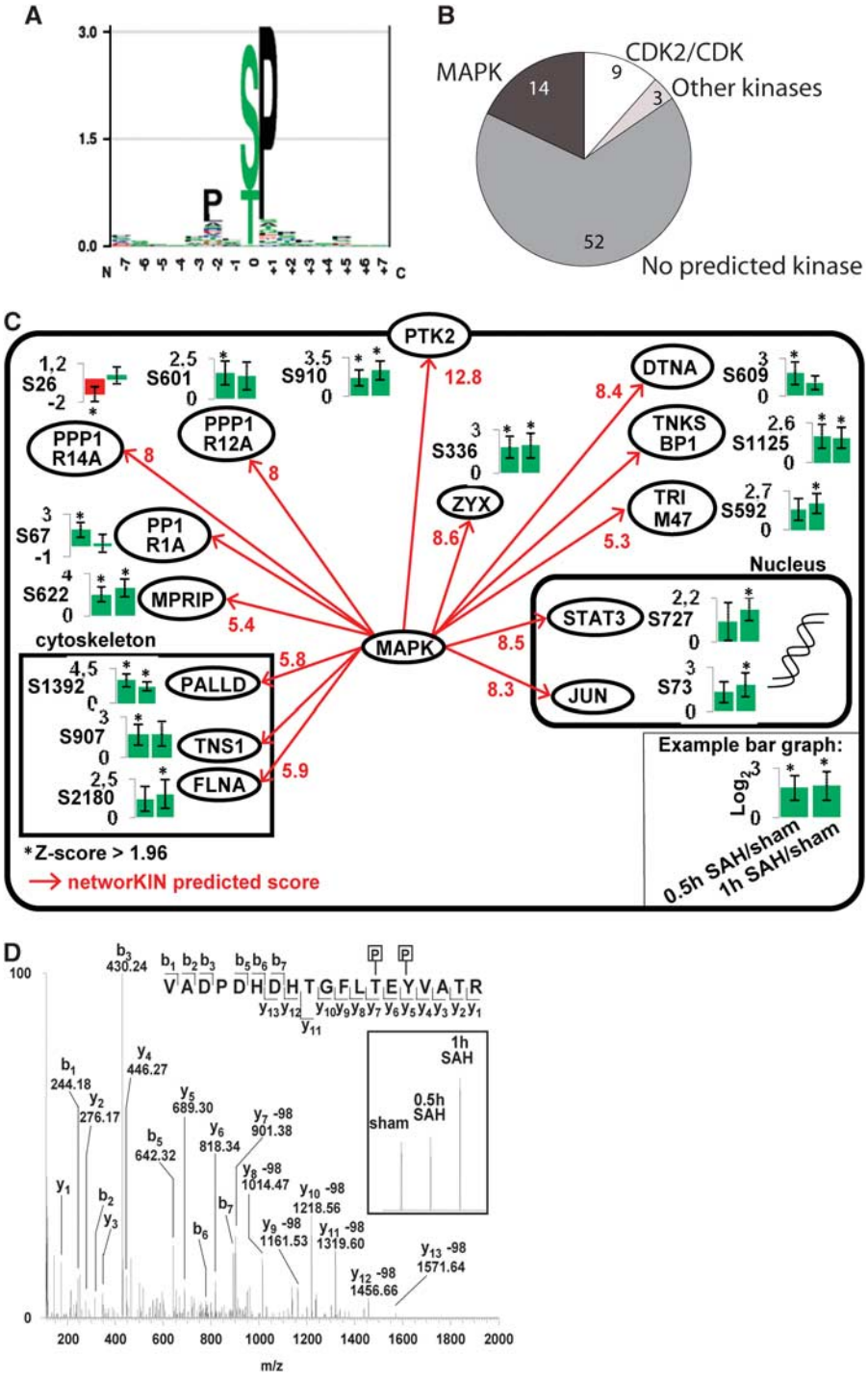

Figure 2. Networking phosphorylation substrate motif analysis. (**A**) P*X*p(S/T)P mitogen-activated protein kinase (MAPK) phosphorylation substrate motif. (**B**) Distribution of predicted phosphorylation substrate motifs among all significantly subarachnoid hemorrhage (SAH)-regulated phosphopeptides. Numbers of phosphosites assigned to each predicted phosphorylation motif are indicated. (**C**) Network of SAH-regulated MAPK phosphorylation sites. (**D**) Annotated mass spectrometry spectrum of phosphopeptide containing phosphorylated Thr-183 and Tyr-185 of MAPK1 (816.687 *m/z* (3 p.p.m.)). Inserts show zoom of stable isotopes for relative quantification.

represents a promising alternative to treatments targeting individual vasculopathological processes, such as the ET_A receptor antagonist, Clazosentan, recently failing a major trial.[24] In contrast to the central role of MEK-ERK1/2 signaling on the regulation of a panel of selected SAH-induced phosphosites investigated in this study, inhibition of CaMKII had only a minor effect on the panel (the only effect seen was a slight inhibition of SAH-induced FAK Tyr397 phosphorylation). However, this does not exclude the possibility that the observed SAH-induced CaMKII activation has a role in SAH-induced cerebral vasculopathy. CaMKII exists in multiple isoforms, and these have been shown to regulate the activation of multiple transcription factors and histone deacetylases in vascular smooth muscle in response to stimulation with e.g., transforming growth factor β[38] and

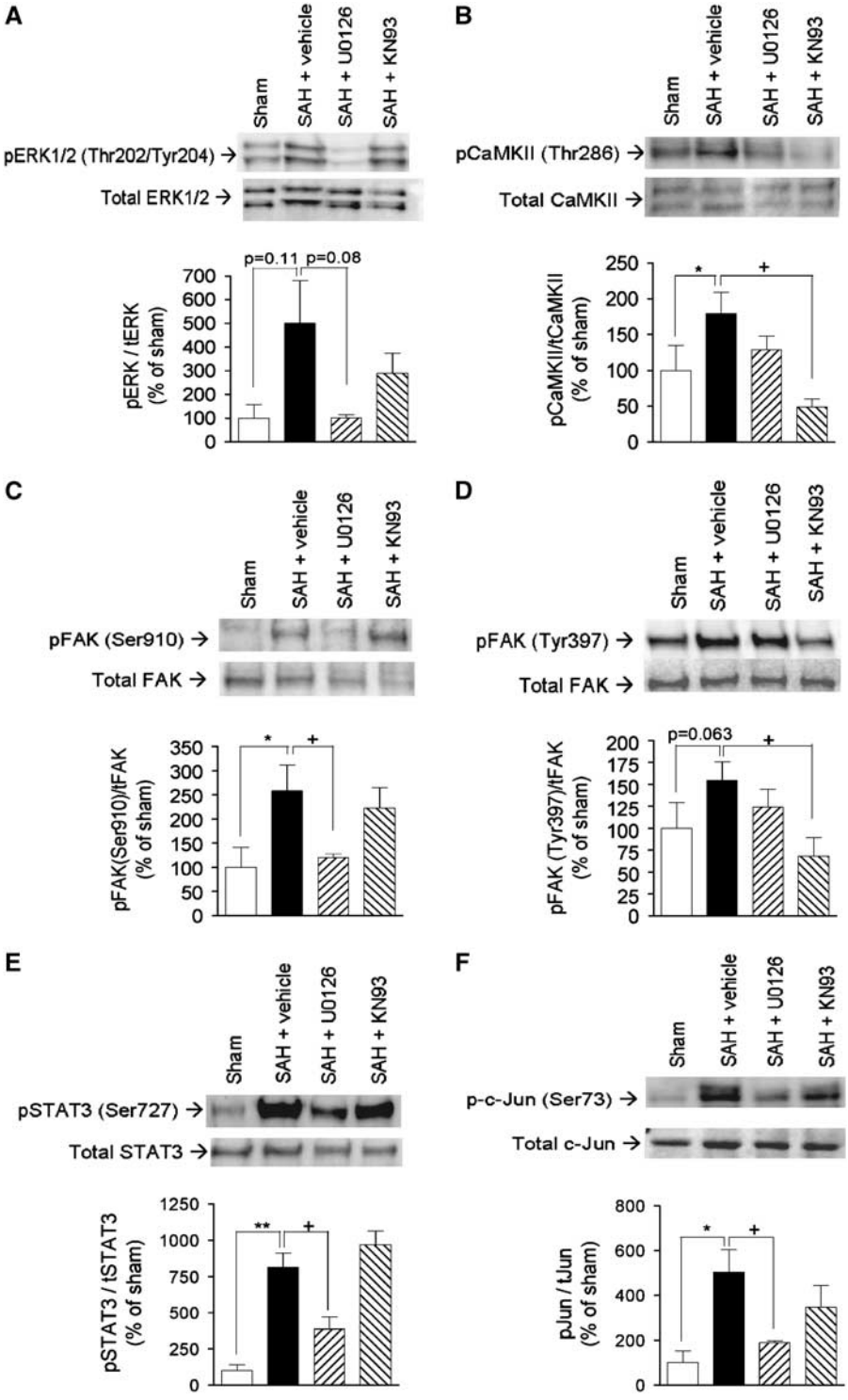

Figure 3. Validation of selected subarachnoid hemorrhage (SAH)-induced phosphorylations and their dependence on extracellular regulated kinase 1/2 and calcium calmodulin-dependent kinase II (CaMKII) activity. (**A**) Phosphorylation of ERK1/2 at Thr202/Thr204, (**B**) phosphorylation of CaMKII at Thr286, (**C**) phosphorylation of FAK at Ser910, (**D**) phosphorylation of FAK at Tyr397, (**E**) phosphorylation of STAT3 at Ser727, (**F**) phosphorylation of c-Jun at Ser73. Each panel shows Western blots of cerebral artery tissue from sham-operated rats (sham) and SAH rats terminated in post SAH treated with either vehicle, mitogen-activated protein kinase kinase inhibitor U0126, or CaMKII inhibitor KN93 in prior to induction of SAH. Each panel shows representative immunoblots (top) and band chemiluminiscence intensity quantifications presented as means ± s.e.m. of the ratios between phosphorylated and total protein amounts for $n = 4$ to 5 rats in each group (bottom). *Significant differences between sham rats and vehicle-treated SAH rats, $^{+}$ significant differences between vehicle- and inhibitor-treated SAH rats.

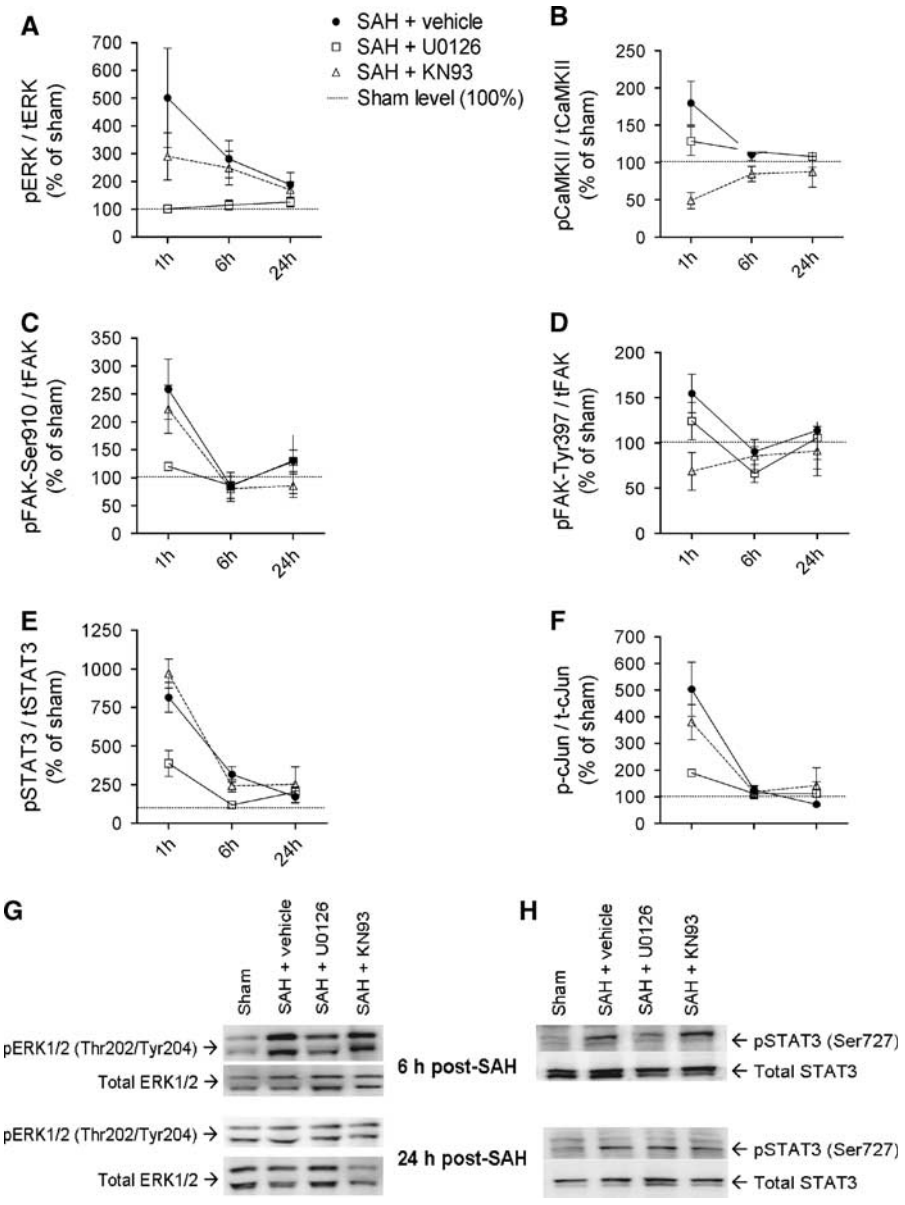

Figure 4. Time course of selected subarachnoid hemorrhage (SAH)-induced phosphorylations and their dependence on extracellular regulated kinase 1/2 (ERK1/2) and calcium calmodulin-dependent kinase II (CaMKII) activity. (**A–F**) Band chemiluminiscence intensity quantifications presented as means ± s.e.m. of the ratios between phosphorylated and total protein amounts for sham-operated rats (set to 100% at each time point) and SAH rats treated with either vehicle, mitogen-activated protein kinase kinaseinhibitor U0126, or CaMKII inhibitor KN93 terminated at 1, 6 or 24 hours after SAH or sham-operation. $n = 4$ to 5 rats in each group. (**G**, **H**) Representative immunoblots of ERK1/2 and signal transducer and activator of transcription phosphorylation in rats terminated 6 or 24 hours after SAH/sham operation.

angiotensin II,[39] the latter leading to vascular smooth muscle hypertrophy. Such transcriptional effects of CaMKII activation could potentially influence cerebrovascular structure and function after SAH via mechanisms not revealed within the time-frame and panel of selected molecules investigated in the present study.

The downstream effectors of ERK1/2 in SAH-induced vasculopathy are not known, but the present study reveals a number of SAH-induced ERK1/2-mediated phosphorylation events, which may all represent important downstream events. One of these is STAT3 that we demonstrate is phosphorylated downstream of ERK1/2 at 1 hour post SAH persisting for at least 24 hour. Transcriptional activation by STAT3 involves phosphorylation of two sites: Tyr705 necessary for STAT3 dimerization, nuclear translocation and DNA binding, and Ser727 enhancing recruitment of necessary transcriptional cofactors.[40] An earlier study using an SAH model with blood injection in cisterna magna showed phosphorylation of STAT3 only at Tyr705 at 2 hours post SAH, extending to Ser727 at day 1 to 2 post SAH,[41] whereas we show strong Ser727 phosphorylation at 1 hour post SAH, declining to a lower level at 6 hours and 24 hours post SAH, where it is accompanied by Tyr705 phosphorylation. Regardless of the exact sequence of STAT3 phosphorylations, both studies demonstrate early STAT3 activation in cerebral arteries after SAH. STAT3 phosphorylation on Tyr705 can be induced by Janus kinases and Src non-receptor tyrosine kinases, whereas Ser727 phosphorylation is typically downstream of MAPKs.[40] Thus, STAT3 Ser727 phosphorylation downstream of ERK1/2 has been demonstrated in numerous cell types,[42–44] and ERK1/2 is thought to be a bona fide STAT3 kinase targeting Ser727. Accordingly, we show that SAH-induced STAT3 Ser727 phosphorylation in cerebral

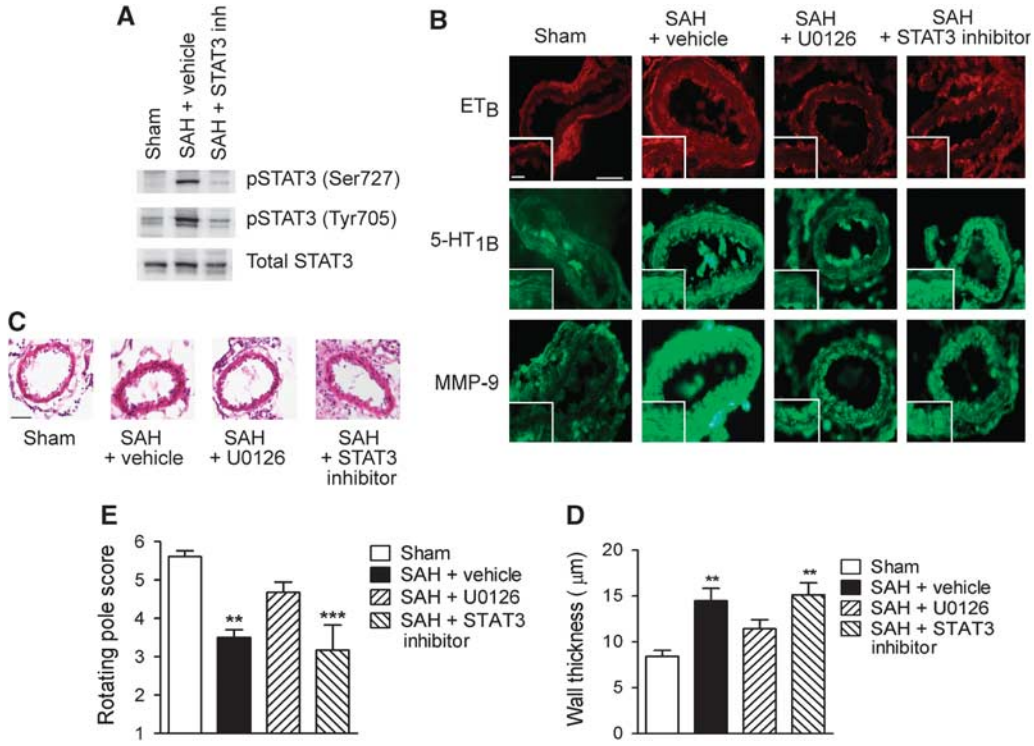

Figure 5. Effect of inhibition of mitogen-activated protein kinase kinase (MEK1/2) or signal transducer and activator of transcription (STAT3) on cerebral vasculopathy and neurologic outcome. (**A**) Validation of STAT3 inhibitor activity in cerebral arteries after intracranial administration. Representative western blots showing levels of phosphorylated and total STAT3 in cerebral arteries from sham-operated and subarachnoid hemorrhage (SAH) rats (treated with vehicle or STAT3 inhibitor) terminated 24 hours post surgery. (**B**) Immunohistochemical stainings showing expression of ET_B and 5-HT_{1B} receptors and MMP-9. Shown are representative sections of middle cerebral arteries from sham-operated rats and SAH rats treated with either vehicle, the MEK1/2 inhibitor U0126, or STAT3 inhibitor. Inserts show magnification of vessel wall to illustrate smooth muscle staining. Scale bar in large image is 50 μm, scale bar in insert is 20 μm. (**C**) Hematoxylin-eosin stainings of middle cerebral artery sections from sham-operated rats and SAH rats treated with vehicle, U0126, or STAT3 inhibitor. Scale bar is 50 μm. (**D**) Quantifications of wall thicknesses. Data are means ± s.e.m. of average thicknesses of four to six animals in each group. Stars indicate significant differences as compared with sham-operated rats determined by one-way analysis of variance (ANOVA) with Bonferroni's post test. $^{**}P<0.01$. (**E**) Rotating pole test scores of sham-operated rats and SAH rats treated with vehicle, U0126, or STAT3 inhibitor. Data are means ± s.e.m. of average scores for six animals in each group ($n=6$). *** indicates significant differences as compared with sham-operated rats determned by one-way ANOVA with Bonferroni's post test. $^{**}P<0.01$, $^{***}P<0.001$.

arteries is ERK1/2-dependent; however, our data do not allow us to conclude on further upstream events. The two STAT3 phosphorylation events (Ser772 and Tyr705) may be induced downstream of separate or common upstream events, and they may be regulated by different upstream events at different time points post SAH.

We investigated STAT3 as a possible downstream alternative to direct targeting of the MEK-ERK1/2 pathway, perhaps less prone to adverse effects. This is, to our knowledge, the first study to evaluate the effects of a STAT3 inhibitor in an SAH model. However, STAT3 inhibition only partially mimicked the effect of MEK–ERK1/2 inhibition on expressional changes in cerebral arteries after SAH. Most importantly, STAT3 inhibition did not, like MEK1/2 inhibition, reduce cerebral artery wall thickness and neurologic deficits, suggesting that the broad effect of MEK1/2 inhibition on a range of proteins involved in cerebral vasculopathy is central for improving these composite endpoints.

In conclusion, our data reveal a strong acute SAH-induced regulation of focal adhesion complexes and actin cytoskeleton dynamics as well as activation of a number of kinases and transcription factors in cerebral artery tissue. Our follow-up analysis highlights the MEK–ERK1/2 pathway as a promising therapeutic target for prevention of delayed vasculopathy and cerebral ischemia after SAH. Moreover, our data suggest that STAT3 functions as a downstream mediator of some, but not all, vasculopathological changes triggered by ERK1/2 activation. Finally, this study reveals the feasibility, power, and utility of a phosphoproteomic approach to studies of cerebrovascular injury.

DISCLOSURE/CONFLICT OF INTEREST

The authors declare no conflict of interest.

ACKNOWLEDGEMENTS

We thank Lene Jakobsen and Kasper Engholm-Keller for instrument maintenance and help with HILIC, respectively. We thank Dr Karin Warfvinge for help with the immunohistochemistry.

REFERENCES

1 Vergouwen MD, Ilodigwe D, Macdonald RL. Cerebral infarction after subarachnoid hemorrhage contributes to poor outcome by vasospasm-dependent and -independent effects. *Stroke* 2011; **42**: 924–929.
2 Dumont AS, Dumont RJ, Chow MM, Lin CL, Calisaneller T, Ley KF *et al.* Cerebral vasospasm after subarachnoid hemorrhage: putative role of inflammation. *Neurosurgery* 2003; **53**: 123–135.
3 Kozniewska E, Michalik R, Rafalowska J, Gadamski R, Walski M, Frontczak-Baniewicz M *et al.* Mechanisms of vascular dysfunction after subarachnoid hemorrhage. *J Physiol Pharmacol* 2006; **57**(Suppl 11): 145–160.

4 Edvinsson LI, Povlsen GK. Vascular plasticity in cerebrovascular disorders. *J Cereb Blood Flow Metab* 2011; **31**: 1554–1571.
5 Beg SH-S J, Vikman P, Xu CB, Edvinsson L. Protein kinase C inhibition prevents upregulation of vascular ET(B) and 5-HT(1B) receptors and reverses cerebral blood flow reduction after subarachnoid hemorrhage in rats. *J Cereb Blood Flow Metab* 2007; **27**: 21–32.
6 Yamaguchi M, Zhou C, Nanda A, Zhang JH. Ras protein contributes to cerebral vasospasm in a canine double-hemorrhage model. *Stroke* 2004; **35**: 1750–1755.
7 Larsen CC, Povlsen GK, Rasmussen MN, Edvinsson L. Improvement in neurological outcome and abolition of cerebrovascular endothelin B and 5-hydroxytryptamine 1B receptor upregulation through mitogen-activated protein kinase kinase 1/2 inhibition after subarachnoid hemorrhage in rats. *J Neurosurg* 2010; **114**: 1143–1153.
8 Chen D, Wei XT, Guan JH, Yuan JW, Peng YT, Song L *et al.* Inhibition of c-Jun N-terminal kinase prevents blood-brain barrier disruption and normalizes the expression of tight junction proteins clautin-5 and ZO-1 in a rat model of subarachnoid hemorrhage. *Acta Neurochir (Wien)* 2012; **154**: 1469–1476.
9 Zhang X, Zhao XD, Shi JX, Yin HX. Inhibition of the p38 mitogen-activated protein kinase (MAPK) pathway attenuates cerebral vasospasm following experimental subarachnoid hemorrhage in rabbits. *Ann Clin Lab Sci* 2011; **41**: 244–250.
10 Choudhary C, Mann M. Decoding signalling networks by mass spectrometry-based proteomics. *Nat Rev Mol Cell Biol* 2010; **11**: 427–439.
11 Larsen MR, Thingholm TE, Jensen ON, Roepstorff P, Jorgensen TJ. Highly selective enrichment of phosphorylated peptides from peptide mixtures using titanium dioxide microcolumns. *Mol Cell Proteomics* 2005; **4**: 873–886.
12 Engholm-Keller K, Birck P, Storling J, Pociot F, Mandrup-Poulsen T, Larsen MR. TiSH—a robust and sensitive global phosphoproteomics strategy employing a combination of TiO(2), SIMAC, and HILIC. *J Proteomics* 2012; **75**: 5749–5761.
13 Savitski MM, Lemeer S, Boesche M, Lang M, Mathieson T, Bantscheff M *et al.* Confident phosphorylation site localization using the Mascot Delta Score. *Mol Cell Proteomics* 2011; **10**: M110.003830.
14 Toedling J, Skylar O, Krueger T, Fischer JJ, Sperling S, Huber W. Ringo--an R/Bioconductor package for analyzing ChIP-chip readouts. *BMC Bioinformatics* 2007; **8**: 221.
15 Yang I, Chen E, Hasseman J, Liang W, Frank B, Wang S *et al.* Within the fold: assessing differential expression measures and reproducibility in microarray assays. *Genome Biol* 2002; **3**: research0062.0061—research0062.0012.
16 Karp NA, Huber W, Sadowski PG, Charles PD, Hester SV, Lilley KS. Addressing accuracy and precision issues in iTRAQ quantitation. *Mol Cell Proteomics* 2010; **9**: 1885–1897.
17 Linding R, Jensen LJ, Ostheimer GJ, van Vugt MA, Jorgensen C, Miron IM *et al.* Systematic discovery of *in vivo* phosphorylation networks. *Cell* 2007; **129**: 1415–1426.
18 Cipolletta E, Monaco S, Maione AS, Vitiello L, Campiglia P, Pastore L *et al.* Calmodulin-dependent kinase II mediates vascular smooth muscle cell proliferation and is potentiated by extracellular signal regulated kinase. *Endocrinology* 2010; **151**: 2747–2759.
19 Lehoux S, Tedgui A. Signal transduction of mechanical stresses in the vascular wall. *Hypertension* 1998; **32**: 338–345.
20 Lufei C, Koh TH, Uchida T, Cao X. Pin1 is required for the Ser727 phosphorylation-dependent Stat3 activity. *Oncogene* 2007; **26**: 7656–7664.
21 Pulverer BJ, Kyriakis JM, Avruch J, Nikolakaki E, Woodgett JR. Phosphorylation of c-jun mediated by MAP kinases. *Nature* 1991; **353**: 670–674.
22 Waldsee R, Ahnstedt H, Eftekhari S, Edvinsson L. Involvement of calcium-calmodulin-dependent protein kinase II in endothelin receptor expression in rat cerebral arteries. *Am J Physiol Heart Circ Physiol* 2010; **298**: H823–H832.
23 Dhar R, Diringer M. Statins and anti-inflammatory therapies for subarachnoid hemorrhage. *Curr Treat Options Neurol* 2012; **14**: 164–174.
24 Macdonald RL, Higashida RT, Keller E, Mayer SA, Molyneux A, Raabe A *et al.* Randomized trial of clazosentan in patients with aneurysmal subarachnoid hemorrhage undergoing endovascular coiling. *Stroke* 2012; **43**: 1463–1469.
25 Qi YX, Jiang J, Jiang XH, Wang XD, Ji SY, Han Y *et al.* PDGF-BB and TGF-{beta}1 on cross-talk between endothelial and smooth muscle cells in vascular remodeling induced by low shear stress. *Proc Natl Acad Sci USA* 2011; **108**: 1908–1913.
26 Kim HK, Park WS, Warda M, Park SY, Ko EA, Kim MH *et al.* Beta adrenergic overstimulation impaired vascular contractility via actin-cytoskeleton disorganization in rabbit cerebral artery. *PLoS One* 2012; **7**: e43884.
27 Kubota K, Anjum R, Yu Y, Kunz RC, Andersen JN, Kraus M *et al.* Sensitive multiplexed analysis of kinase activities and activity-based kinase identification. *Nat Biotechnol* 2009; **27**: 933–940.
28 Xue L, Wang WH, Iliuk A, Hu L, Galan JA, Yu S *et al.* Sensitive kinase assay linked with phosphoproteomics for identifying direct kinase substrates. *Proc Natl Acad Sci USA* 2012; **109**: 5615–5620.
29 Romer LH, Birukov KG, Garcia JG. Focal adhesions: paradigm for a signaling nexus. *Circ Res* 2006; **98**: 606–616.
30 Hunger-Glaser I, Fan RS, Perez-Salazar E, Rozengurt E. PDGF and FGF induce focal adhesion kinase (FAK) phosphorylation at Ser-910: dissociation from Tyr-397 phosphorylation and requirement for ERK activation. *J Cell Physiol* 2004; **200**: 213–222.
31 Li LH, Zheng MH, Luo Q, Ye Q, Feng B, Lu AG *et al.* P21-activated protein kinase 1 induces colorectal cancer metastasis involving ERK activation and phosphorylation of FAK at Ser-910. *Int J Oncol* 2010; **37**: 951–962.
32 Lo SH. Tensin. *Int J Biochem Cell Biol* 2004; **36**: 31–34.
33 te Velthuis AJ, Bagowski CP. PDZ and LIM domain-encoding genes: molecular interactions and their role in development. *ScientificWorldJournal* 2007; **7**: 1470–1492.
34 Hervy M, Hoffman L, Beckerle MC. From the membrane to the nucleus and back again: bifunctional focal adhesion proteins. *Curr Opin Cell Biol* 2006; **18**: 524–532.
35 Cestra G, Toomre D, Chang S, De Camilli P. The Abl/Arg substrate ArgBP2/nArgBP2 coordinates the function of multiple regulatory mechanisms converging on the actin cytoskeleton. *Proc Natl Acad Sci USA* 2005; **102**: 1731–1736.
36 Rasmussen M, Larsen S, Skovsted G, Edvinsson L. Lack of wall tension in rat cerebral arteries cause enhanched endothelin B (ETB) receptor contractile responses. 10th International Symposium on Resistance Arteries, poster P5.02, Rebild, Denmark.
37 Kusaka G, Kimura H, Kusaka I, Perkins E, Nanda A, Zhang JH. Contribution of Src tyrosine kinase to cerebral vasospasm after subarachnoid hemorrhage. *J Neurosurg* 2003; **99**: 383–390.
38 Rezaei HB, Kamato D, Ansari G, Osman N, Little PJ. Cell biology of Smad2/3 linker region phosphorylation in vascular smooth muscle. *Clin Exp Pharmacol Physiol* 2012; **39**: 661–667.
39 Ginnan R, Sun LY, Schwarz JJ, Singer HA. MEF2 is regulated by CaMKIIdelta2 and a HDAC4-HDAC5 heterodimer in vascular smooth muscle cells. *Biochem J* 2012; **444**: 105–114.
40 Decker T, Kovarik P. Serine phosphorylation of STATs. *Oncogene* 2000; **19**: 2628–2637.
41 Osuka K, Watanabe Y, Yamauchi K, Nakazawa A, Usuda N, Tokuda M *et al.* Activation of the JAK-STAT signaling pathway in the rat basilar artery after subarachnoid hemorrhage. *Brain Res* 2006; **1072**: 1–7.
42 Washburn KB, Neary JT. P2 purinergic receptors signal to STAT3 in astrocytes: difference in STAT3 responses to P2Y and P2X receptor activation. *Neuroscience* 2006; **142**: 411–423.
43 Coppo P, Flamant S, De Mas V, Jarrier P, Guillier M, Bonnet ML *et al.* BCR-ABL activates STAT3 via JAK and MEK pathways in human cells. *Br J Haematol* 2006; **134**: 171–179.
44 O'Rourke L, Shepherd PR. Biphasic regulation of extracellular-signal-regulated protein kinase by leptin in macrophages: role in regulating STAT3 Ser727 phosphorylation and DNA binding. *Biochem J* 2002; **364**: 875–879.